Disturbed Ca^{2+} signaling and apoptosis of medium spiny neurons in Huntington's disease

Tie-Shan Tang*, Elizabeth Slow†, Vitalie Lupu*, Irina G. Stavrovskaya‡, Mutsuyuki Sugimori§, Rodolfo Llinás§, Bruce S. Kristal‡¶, Michael R. Hayden†, and Ilya Bezprozvanny*‖

*Department of Physiology, University of Texas Southwestern Medical Center, Dallas, TX 75390; †Center for Molecular Medicine and Therapeutics, Department of Medical Genetics, Children's and Woman's Hospital, University of British Columbia, Vancouver, BC, Canada V6T 1Z4; ‡Dementia Research Service, Burke Medical Research Institute, White Plains, NY 10605; §Department of Physiology and Neuroscience, New York University School of Medicine, New York, NY 10016; and ¶Department of Neuroscience, Weill Medical College of Cornell University, New York, NY 10022

Contributed by Rodolfo Llinás, December 22, 2004

Huntington's disease (HD) is caused by polyglutamine expansion (exp) in huntingtin. Here, we used a yeast artificial chromosome (YAC) transgenic mouse model of HD to investigate the connection between disturbed calcium (Ca^{2+}) signaling and apoptosis of HD medium spiny neurons (MSN). Repetitive application of glutamate elevates cytosolic Ca^{2+} levels in MSN from the YAC128 mouse but not in MSN from the wild-type or control YAC18 mouse. Application of glutamate results in apoptosis of YAC128 MSN but not wild-type or YAC18 MSN. Analysis of glutamate-induced apoptosis of the YAC128 MSN revealed that (*i*) actions of glutamate are mediated by mGluR1/5 and NR2B glutamate receptors; (*ii*) membrane-permeable inositol 1,4,5-trisphosphate receptor blockers 2-APB and Enoxaparin (Lovenox) are neuroprotective; (*iii*) apoptosis involves the intrinsic pathway mediated by release of mitochondrial cytochrome *c* and activation of caspases 9 and 3; (*iv*) apoptosis requires mitochondrial Ca^{2+} overload and can be prevented by the mitochondrial Ca^{2+} uniporter blocker Ruthenium 360; and (*v*) apoptosis involves opening of mitochondrial permeability transition pore (MPTP) and can be prevented by MPTP blockers such as bongkrekic acid, Nortriptyline, Desipramine, Trifluoperazine, and Maprotiline. These findings describe a pathway directly linking disturbed Ca^{2+} signaling and degeneration of MSN in the caudate nucleus in HD. These findings also suggest that Ca^{2+} and MPTP blockers may have a therapeutic potential for treatment of HD.

Enoxaparin | neurodegeneration | transgenic mouse | mitochondria | Lovenox

Huntington's disease (HD) has onset usually between 35 and 50 years with chorea and psychiatric disturbances and gradual but inexorable intellectual decline to death after 15–20 years (1). Neuropathological analysis reveals selective and progressive neuronal loss in the striatum (1), particularly affecting the GABAergic medium spiny neurons (MSN). At the molecular level, the cause of HD is a polyglutamine expansion (exp) in the amino terminus of huntingtin (Htt), a 350-kDa ubiquitously expressed cytoplasmic protein (2). Despite significant progress, cellular mechanisms that link the Htt^{exp} mutation with the disease are poorly understood (3).

A number of transgenic HD mouse models have been generated that reproduce many HD-like features (4). In the yeast artificial chromosome (YAC128) mouse model, the full-length human Htt protein with polyglutamine exp (128Q) is expressed under the control of its endogenous promoter and regulatory elements (5). The onset of a motor deficit before striatal neuronal loss in the YAC128 mouse model accurately recapitulates the progression of HD (5). Thus, the YAC128 mouse model is ideal for understanding the cellular mechanisms that lead to neurodegeneration in HD, as well as for validating potential therapeutic agents.

Previous studies demonstrated that Htt^{exp} facilitates activity of the NR2B subtype of NMDA receptors (NMDARs) (6–8) and the type 1 inositol 1,4,5-trisphosphate receptors ($InsP_3R1$) (9). A connection between disturbed Ca^{2+} signaling and neuronal apoptosis is well established (10, 11), and we therefore proposed that Htt^{exp}-induced Ca^{2+} overload results in degeneration of MSN in HD (12). To test this hypothesis, we analyzed Ca^{2+} signals and apoptotic cell death in primary cultures of MSN from the YAC128 mice. Our results provide further support to the hypothesis that disturbed Ca^{2+} underlies neuronal cell death in HD (12) and allowed us to identify a number of potential therapeutic targets for HD treatment.

Materials and Methods

Primary Neuronal Cultures. Generation and breeding of YAC18 and YAC128 transgenic mice (FVBN/NJ background strain) are described in refs. 5 and 13. Heterozygous male YAC128 or YAC18 mice were crossed with the wild-type (WT) female mice and resulting litters were collected at postnatal days 1–2. The pups were genotyped by PCR with primers specific for exons 44 and 45 of human Htt gene and the medium spiny neuronal (MSN) or hippocampal neuronal (HN) cultures of WT, YAC18, and YAC128 mice were established and maintained as described in ref. 9.

Ca^{2+} Imaging Experiments. Fura-2 Ca^{2+} imaging experiments with 14- to 16-DIV (days *in vitro*) MSN cultures were performed as described in ref. 9, using a DeltaRAM illuminator, an IC-300 camera, and IMAGEMASTER PRO software (all from PTI, South Brunswick, NJ). The cells were maintained in artificial cerebrospinal fluid (aCSF) (140 mM NaCl/5 mM KCl/1 mM $MgCl_2$/2 mM $CaCl_2$/10 mM Hepes, pH 7.3) at 37°C during measurements (PH1 heater, Warner Instruments, Hamden, CT). Fura-2 340/380 ratio images were collected every 6 sec for the duration of the experiment. Baseline (1–3 min) measurements were obtained before first pulse of glutamate. The 20 μM glutamate solution was dissolved in aCSF and 1-min pulses of 37°C glutamate solution (SH-27B in-line solution heater, Warner Instruments) were applied by using a valve controller (VC-6, Warner Instruments) driven by a square-pulse electrical waveform generator (Model 148A, Wavetek, San Diego). DHPG (3,5-dihydroxyphenylglycine)-induced Ca^{2+} responses have been measured in Ca^{2+}-free aCSF (omitted $CaCl_2$ from aCSF and supplemented with 100 μM EGTA). For the Enoxaparin experiments, MSN were preincubated in medium containing 200

Abbreviations: CPCCOEt, 7-(hydroxyimino)cyclopropa[*b*]chromen-1a-carboxylate ethyl ester; DIV, days *in vitro*; exp, expansion; HD, Huntington's disease; Htt, huntingtin; $InsP_3$, inositol 1,4,5-trisphosphate; $InsP_3R1$, type 1 $InsP_3$ receptor; MCU, mitochondrial Ca^{2+} uniporter/channel; MPEP, 2-methyl-6-(phenylethynyl)pyridine hydrochloride; MPTP, mitochondrial permeability transition pore; MSN, medium spiny neurons; NMDAR, NMDA receptor; PI, propidium iodide; Ru360, Ruthenium 360.

‖To whom correspondence should be addressed at: Department of Physiology, K4.112, University of Texas Southwestern Medical Center, Dallas, TX 75390-9040. E-mail: ilya.bezprozvanny@utsouthwestern.edu.

www.pnas.org/cgi/doi/10.1073/pnas.0409402102

μg/ml Enoxaparin for 3 h. Enoxaparin was included at 200 μg/ml in all solutions during Fura-2 loading and Ca^{2+} imaging steps.

TUNEL Staining Experiments. The 14-DIV MSN or HN were exposed for 8 h to a range of glutamate concentrations added to the culture medium. During exposure to glutamate, the cells were maintained in a cell culture incubator (humidified 5% CO_2, 37°C). (+)MK-801, ifenprodil, MPEP [2-methyl-6-(phenylethynyl)pyridine hydrochloride], CPCCOEt {7-(hydroxyimino)cyclopropa[*b*]chromen-1a-carboxylate ethyl ester}, and Ruthenium (Ru) 360 were added to cell culture media 30 min before the addition of glutamate. 2-APB, Enoxaparin, Z-VAD-FMK, Z-FA-FMK, Z-DEVD-FMK, Z-LEHD-FMK, Z-IETD-FMK, bongkrekic acid, Nortriptyline, Pirenzepine, Promethazine, Desipramine, Trifluoperazine, Thiothixene, and Maprotiline were added 2–3 h before glutamate exposure. Immediately after exposure to glutamate, neurons were fixed for 30 min in 4% paraformaldehyde plus 4% sucrose in PBS (pH 7.4), permeabilized for 5 min in 0.25% Triton X-100, and stained by using the DeadEnd Fluorometric TUNEL System (Promega) according to the manufacturer's instructions. Nuclei were counterstained with 5 μM propidium iodide (PI) (Molecular Probes). Coverslips were extensively washed with PBS and mounted in Mowiol 4-88 (Polysciences). FITC- and PI-fluorescent images were collected with an Olympus IX70 microscope with ×40 objectives, using a Cascade:650 camera (Roper Scientific) and METAFLUOR software (Universal Imaging, Downingtown, PA). Four to six randomly chosen microscopic fields containing 200–300 MSN were captured, and the number of TUNEL-positive neuronal nuclei was calculated as a fraction of PI-positive neuronal nuclei in each microscopic field by an observer blinded to the nature of the sample. Nuclei of glial cells, identified by large size and weak PI staining, were not counted in the analysis. The fractions of TUNEL-positive nuclei determined for each microscopic field were averaged, and the results are presented as means ± SD (n = number of fields counted).

Planar Lipid Bilayer Experiments. Single-channel recordings of rat cerebellar $InsP_3R1$ were performed as described in ref. 14. Briefly, rat cerebellar microsomes were isolated by differential centrifugation and fused to planar lipid bilayers. The activity of $InsP_3$-gated channels was recorded at a 0-mV transmembrane potential by using 50 mM Ba^{2+} (trans) dissolved in Hepes (pH 7.35) as a charge carrier. The cis (cytosolic) chamber contained 110 mM Tris dissolved in Hepes (pH 7.35), 0.5 mM Na_2ATP, and pCa 6.7 (0.2 mM EGTA plus 0.14 mM $CaCl_2$). Cerebellar $InsP_3R1$ was activated by addition of 2 μM $InsP_3$ (Alexis) to the cis chamber. Different concentrations of Enoxaparin were added to the cis chamber. The $InsP_3$-gated currents were amplified (OC-725, Warner Instruments), filtered at 1 kHz by low-pass 8-pole Bessel filter, digitized at 5 kHz (Digidata 1200, Axon Instruments), and stored on a computer hard drive and optical discs. For off-line computer analysis (PCLAMP 6, Axon Instruments), currents were filtered digitally at 500 Hz. For presentation of the current traces, data were filtered at 200 Hz.

Cytochrome *c* Release Assay. MSN cultures at 12- to 14-DIV were exposed to glutamate for 5 h, washed once with PBS, scraped off in the homogenization buffer (0.32 M sucrose/25 mM Hepes, pH 8.0/1 mM EDTA/1 mM DTT/protease inhibitors), homogenized, and clarified by a 60-min spin at 100,000 × g. The supernatant was collected as the soluble fraction, and the protein concentration of each sample was determined by using a Bio-Rad protein assay kit. Both pellet and supernatant were lysed in SDS-loading buffer and boiled. Samples were resolved by SDS/PAGE, analyzed by Western blotting with anti-cytochrome c monoclonal antibody (BD Pharmingen), and quantified by densitometry.

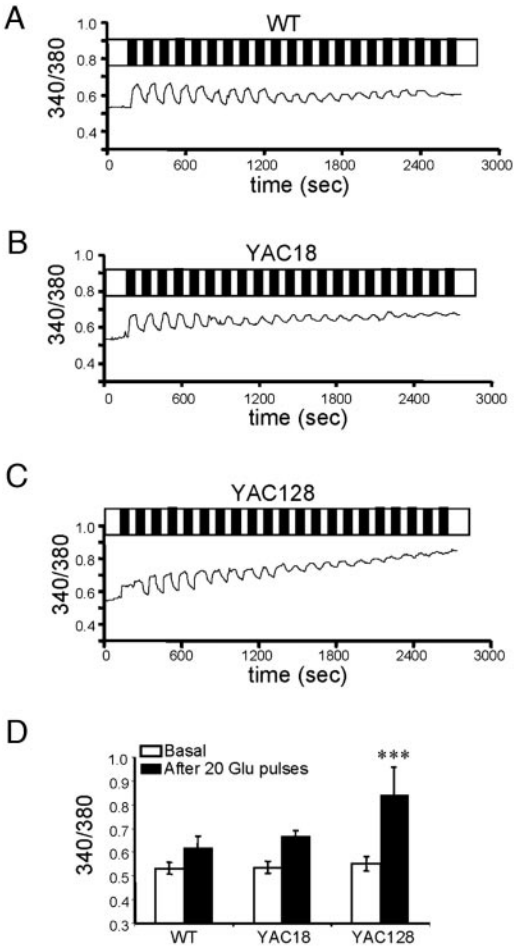

Fig. 1. Deranged Ca^{2+} signaling in YAC128 MSN. (*A–C*) Repetitive application of 20 μM glutamate induces Ca^{2+} signals in MSN from the WT (*A*), YAC18 (*B*), and YAC128 (*C*) mice. Cytosolic Ca^{2+} levels are presented as a 340/380 Fura-2 ratio. Each pulse of glutamate is shown as a black bar (1 min), and the washout step is shown by a white bar (1 min) above the Ca^{2+} trace. The traces shown are average traces from all MSN for each experimental group. (*D*) The average 340/380 values (mean ± SD) before and after 20 pulses of glutamate are shown for WT (n = 50), YAC18 (n = 18), and YAC128 (n = 40) MSN as indicated. After 20 pulses of glutamate the Ca^{2+} levels in YAC128 MSN are significantly (***, $P < 0.05$) higher than those in WT or YAC18 MSN.

Drugs. Ru360 and 2-APB were from Calbiochem. Glutamate, MPEP, CPCCOEt, (+)-MK801 maleate, and ifenprodil were purchased from Tocris. Z-VAD-FMK, Z-FA-FMK, Z-DEVD-FMK, Z-LEHD-FMK, and Z-IETD-FMK were from R & D Systems. Bongkrekic acid, Nortriptyline, Pirenzepine, Promethazine, Desipramine, Trifluoperazine, Thiothixene, and Maprotiline were from Sigma-Aldrich.

Results

Disturbed Ca^{2+} Signals in YAC128 MSN. Previous findings (6–9) suggested that glutamate should induce supranormal Ca^{2+} responses in HD MSN. To test this hypothesis, we compared glutamate-induced Ca^{2+} signals in MSN primary cultures established from the WT, YAC18 (13), and YAC128 (5) mice. To mimic physiological conditions more closely, we applied repetitive pulses of 20 μM glutamate 1 min in duration, followed by a 1-min washout (Fig. 1). The intracellular Ca^{2+} concentration

NEUROSCIENCE

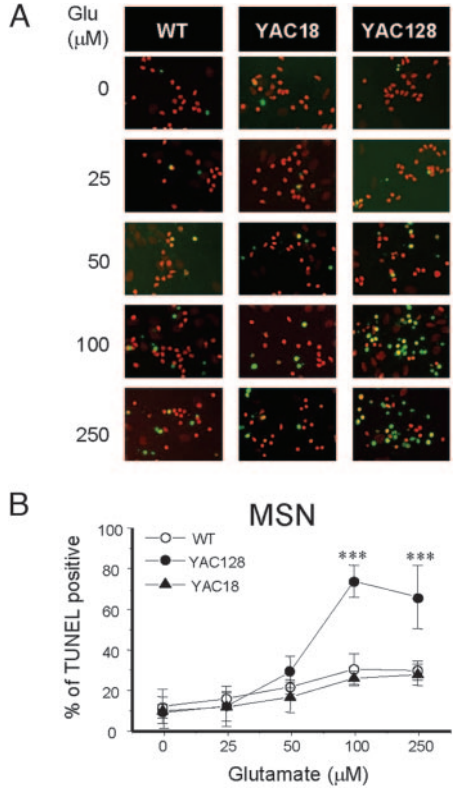

Fig. 2. *In vitro* HD assay. (*A*) Fourteen-DIV MSN from WT, YAC18, and YAC128 mice were exposed to a range of glutamate concentrations for 8 h, fixed, permeabilized, and analyzed by TUNEL staining (green) and PI counterstaining. (*B*) The fraction of TUNEL-positive MSN nuclei was determined as shown in *A* and plotted against glutamate concentration for WT (open circles), YAC128 (filled circles), and YAC18 (filled triangles) mice. At each glutamate concentration, the data are shown as mean ± SD ($n = 4–6$ microscopic fields, 200–300 MSN per field). At 100 and 250 μM glutamate, the fraction of TUNEL-positive MSN is significantly ($P < 0.05$) higher for YAC128 than for WT or YAC18. Similar results were obtained with 10 independent MSN preparations.

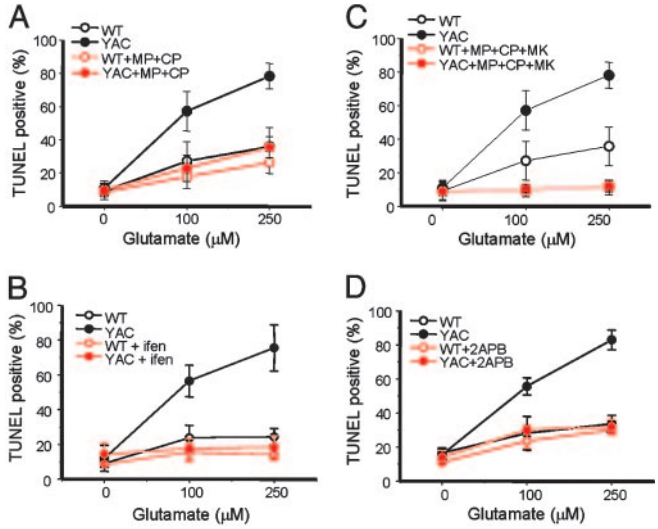

Fig. 3. Ca^{2+} blockers prevent apoptosis of YAC128 MSN. Fourteen-DIV MSN were exposed to a range of glutamate concentrations for 8 h, fixed, permeabilized, and analyzed by TUNEL staining as described in the legend of Fig. 2. The fraction of TUNEL-positive MSN nuclei is plotted against glutamate concentration for WT (open circles) and YAC128 (YAC, filled circles) mice. At each glutamate concentration, the data are shown as mean ± SD ($n = 4–6$ microscopic fields, 200–300 MSN per field). The results in the absence (black symbols) and presence (red symbols) of Ca^{2+} blockers are compared. (*A*) Twenty micromolar MPEP and 50 μM CPCCOEt (mGluR1/5 blockers) were added 30 min before application of glutamate. (*B*) Twenty micromolar ifenprodil (NR2B blocker) was added 30 min before application of glutamate. Similar results were obtained with 10 μM (+)-MK801 (NMDAR blocker). (*C*) Twenty micromolar MPEP, 50 μM CPCCOEt, and 10 μM (+)MK801 were added 30 min before application of glutamate. (*D*) Four hundred micromolar 2-APB (membrane-permeable $InsP_3R$ blocker) was added 3 h before application of glutamate. For *A–D*, in control conditions YAC128 MSN cell death is significantly ($P < 0.05$) higher than WT MSN cell death at 100 and 250 μM glutamate. For *A–D*, in the presence of the drugs YAC128 MSN cell death and WT MSN cell death are not significantly different from each other. Results shown in *A–D* were repeated with two to three independent MSN preparations.

in these experiments was continuously monitored by Fura-2 imaging, and the data were presented as 340/380 ratios (Fig. 1). On average, basal Ca^{2+} levels before glutamate application were not significantly different from each other for all three groups of MSN (Fig. 1*D*). Thus, increase in basal rat and mouse MSN Ca^{2+} levels as a result of Htt overexpression observed in our previous experiments (9, 15) most likely results from high levels of Htt expression in transfected MSN. Repetitive pulses of glutamate caused large elevation of Ca^{2+} levels in the YAC128 MSN (Fig. 1*C*), versus much smaller Ca^{2+} increases in the WT (Fig. 1*A*) and YAC18 (Fig. 1*B*) MSN. On average, Ca^{2+} levels after 20 pulses of glutamate were not significantly different between WT and YAC18 MSN but were significantly ($P < 0.05$) higher in YAC128 MSN when compared with either WT or YAC18 MSN (Fig. 1*D*).

***In Vitro* HD Model.** Next, we established an "*in vitro* HD" model that reproduces Htt^{exp}-dependent degeneration of MSN. These experiments were performed with primary cultures of WT, YAC18, and YAC128 MSN. At 14 DIV, all three groups of MSN were challenged by an 8-h application of glutamate (from 0 to 250 μM) to mimic physiological stimulation. After exposure to glutamate, MSN were fixed, permeabilized, and scored for apoptotic cell death by using TUNEL staining. We determined that, in basal conditions (no glutamate added), ≈10% of MSN in all three experimental groups were apoptotic (TUNEL-positive) (Figs. 2 *A* and *B*). Addition of 25 or 50 μM glutamate increased the number of apoptotic cells to 15–20% in all three experimental groups (Figs. 2 *A* and *B*). Addition of 100 or 250 μM glutamate increased apoptotic death to 60–70% for YAC128 MSN (Figs. 2 *A* and *B*) but only to 25–30% for WT and YAC18 MSN (Figs. 2 *A* and *B*). Thus, we reasoned that exposure to glutamate concentrations in the 100–250 μM range leads to selective apoptosis of YAC128 MSN. As an additional control for specificity of observed degeneration, we compared glutamate-induced apoptosis in primary cultures of WT and YAC128 hippocampal neurons (HN), which are spared in HD (1). No significant differences in apoptosis of HN from WT and YAC128 mice in the 0–500 μM range of glutamate concentrations (8-h exposure) were apparent (data not shown).

Disturbed Ca^{2+} Signaling and Degeneration of MSN in HD. To test the connection between disturbed Ca^{2+} signaling (Fig. 1) and glutamate-induced degeneration of YAC128 MSN (Fig. 2), we assessed the previously described "*in vitro* HD" assay in the presence of Ca^{2+} signaling blockers. We found that inhibition of mGluR1/5 receptors (by a mixture of MPEP and CPCCOEt) reduced the glutamate-induced apoptosis of YAC128 MSN to WT MSN levels (Fig. 3*A*). Inhibition of the NMDAR by (+)MK801 had a similar neuroprotective effect (data not shown). The NR2B-specific antagonist ifenprodil also decreased glutamate-induced apoptosis of YAC128 MSN to WT MSN levels (Fig. 3*B*). A combination of mGluR1/5 and NMDAR

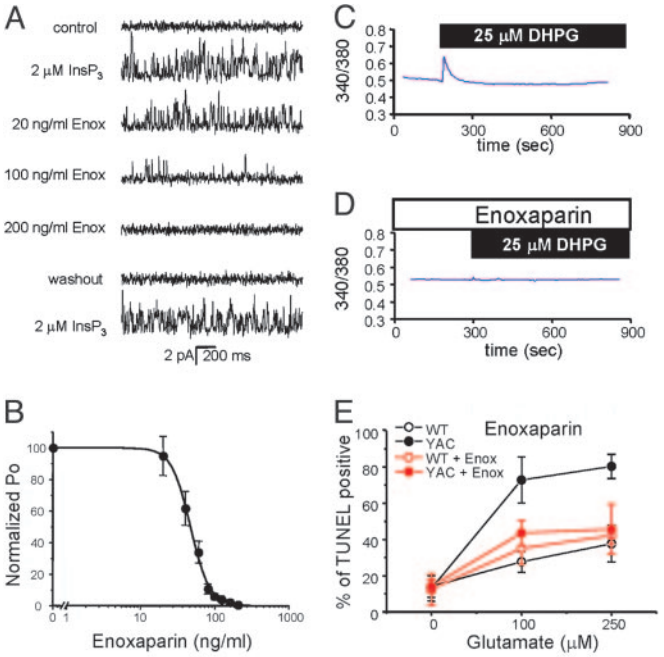

Fig. 4. Enoxaparin protects YAC128 MSN from apoptosis. (*A*) Enoxaparin reversibly inhibits the activity of cerebellar $InsP_3R1$ in planar lipid bilayers. Each current trace corresponds to 2 sec of current recording from the same experiment. $InsP_3$-gated channels in bilayers were activated by 2 μM $InsP_3$ (second trace). Enoxaparin was added to planar lipid bilayers in final concentrations shown next to the third, fourth, and fifth traces. Enoxaparin and $InsP_3$ solutions were removed by perfusion (washout, sixth trace). The $InsP_3$-gated channels in bilayers were reactivated by addition of 2 μM $InsP_3$ (seventh trace). Similar results were obtained in 10 independent experiments. (*B*) The $InsP_3R1$ open probability (P_o) in the presence of 2 μM $InsP_3$ and different Enoxaparin concentrations was determined. For each experiment, the obtained results were normalized to P_o in the same experiment in the absence of Enoxaparin. The normalized data from four independent experiments were averaged together and are shown as means ± SD (filled circles). The normalized and averaged data were fit by the equation $P = 1/(1 + ([Enox]/IC_{50})^n)$. The best fit to the data (smooth curve) yielded an IC_{50} of 50 ng/ml and a Hill coefficient of 3.4. (*C* and *D*) Ca^{2+} responses induced by 25 μM DHPG in Ca^{2+}-free medium in control MSN (*C*, $n = 19$) and in MSN preincubated with 200 μg/ml Enoxaparin for 3 h (*D*, $n = 50$). The average traces are shown for all MSN in the group. (*E*) Enoxaparin at 200 μg/ml was added to WT and YAC128 (YAC) 14-DIV MSN 3 h before glutamate application. The results of TUNEL staining were quantified and are presented as described in the legend of Fig. 3. Cell death of YAC128 MSN is significantly ($P < 0.05$) reduced by the addition of Enoxaparin at 100 and 250 μM glutamate concentrations. Similar results were obtained with two independent MSN preparations.

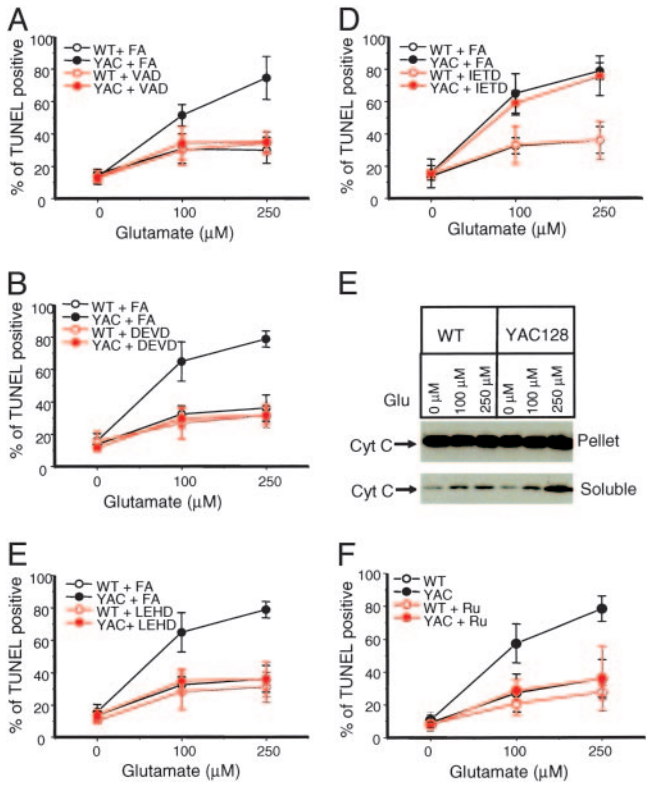

Fig. 5. Apoptosis of YAC128 MSN is mediated by intrinsic pathway. (*A–D*) Membrane-permeable caspase inhibitors were added to 14-DIV WT and YAC128 (YAC) MSN 3 h before the application of glutamate. The results of TUNEL staining were quantified and presented as described in the legend of Fig. 3. The results in the presence of caspase inhibitors (red symbols) and control peptide Z-FA-FMK added in the same concentration (black symbols) are compared. (*A*) Twenty micromolar pan-caspase inhibitor Z-VAD-FMK. (*B*) Fifty micromolar caspase-3 inhibitor Z-DEVD-FMK. (*C*) Fifty micromolar caspase-9 inhibitor Z-LEHD-FMK. (*D*) Fifty micromolar caspase-8 inhibitor Z-IETD-FMK. Cell death of YAC128 MSN is significantly ($P < 0.05$) reduced by the addition of pan-caspase (*A*), caspase-3 (*B*), and caspase-9 (*C*) blockers at 100 and 250 μM glutamate concentrations. Inhibition of caspase-8 (*D*) had no statistically significant effect on cell death of YAC128 MSN at 100 or 250 μM glutamate concentrations. Results shown in *A–D* were repeated with two to three independent MSN preparations. (*E*) Cytochrome *c* release is quantified by Western blotting of mitochondrial (pellet) and cytosolic (soluble) fractions prepared from WT and YAC128 MSN after a 5-h exposure to glutamate. (*F*) Ten micromolar Ru360 was added 30 min before application of glutamate to WT and YAC128 (YAC) MSN. The results of TUNEL staining were quantified and are presented as described in the legend of Fig. 3. Cell death of YAC128 MSN is significantly ($P < 0.05$) reduced by addition of Ru360 at 100 and 250 μM glutamate concentrations.

blockers [MPEP, CPCCOEt, and (+)MK801] completely eliminated glutamate-dependent apoptotic cell death in both WT and YAC128 MSN (Fig. 3*C*). In a previous study, we demonstrated that $InsP_3R1$-mediated Ca^{2+} release is potentiated in MSN transfected with Htt^{exp} expression plasmids (9). Consistent with direct involvement of $InsP_3R1$, preincubation of the MSN cultures with a membrane-permeable $InsP_3R$ blocker 2-APB (16) protected YAC128 MSN from glutamate-induced apoptosis (Fig. 3*D*).

Because $InsP_3R1$ appears to be involved in the glutamate-induced apoptosis of YAC128 MSN (Fig. 3*D*), we hypothesized that $InsP_3R1$ might be a potential drug target for HD treatment. Bath application of a low-molecular-weight heparin sulfate Enoxaparin (Lovenox) prevents glutamate-induced Ca^{2+} release in cerebellar slices, presumably by blocking $InsP_3R1$ activity (17). To directly test the ability of Enoxaparin to block $InsP_3R1$, we performed a series of planar lipid bilayer reconstitution experiments with rat cerebellar microsomes. Addition of Enoxaparin efficiently and reversibly inhibited $InsP_3R1$ in planar lipid bilayers (Fig. 4*A*), similar to actions of a high-molecular-weight heparin. Quantitative analysis of the inhibitory effects of Enoxaparin on $InsP_3R1$ yielded an IC_{50} of 50 ng/ml and a Hill coefficient of 3.4 (Fig. 4*B*), consistent with Enoxaparin binding to each subunit of the $InsP_3R1$ tetramer. To establish that Enoxaparin is able to block $InsP_3R1$ in striatal MSN, we performed a series of Ca^{2+} imaging experiments with Fura-2. As described in ref. 9, application of 25 μM DHPG induced Ca^{2+} release in cultured MSN in Ca^{2+}-free medium (Fig. 4*C*). Preincubation with 200 μg/ml Enoxaparin for 3 h prevented DHPG-induced Ca^{2+} release in cultured MSN (Fig. 4*D*), consistent with the ability of Enoxaparin to permeate cell membranes (17) and block $InsP_3R1$ activity (Figs. 4 *A* and *B*). Using the "*in vitro* HD" assay, we found that 200 μg/ml Enoxaparin protected YAC128 MSN from gluta-

NEUROSCIENCE

Table 1. Effects of putative MPTP blockers on glutamate-induced apoptosis in WT and YAC128 MSN

	WT (% TUNEL-positive)		YAC128 (% TUNEL-positive)	
Drug treatment	100 μM glutamate	250 μM glutamate	100 μM glutamate	250 μM glutamate
Bongkrekic acid				
Control	32.4 ± 11.0	37.3 ± 6.0	66.9 ± 13.1	82.4 ± 9.8
BKA	33.0 ± 6.0	36.0 ± 14.7	39.5 ± 10.3*	41.8 ± 9.9*
Group 1				
Control	30.2 ± 6.0	36.7 ± 16.8	51.4 ± 10.8	75.8 ± 9.6
Nortriptyline	20.9 ± 15.0	36.8 ± 10.8	34.6 ± 7.1*	44.8 ± 13.7*
Pirenzepine	50.3 ± 5.3	49.5 ± 4.1	58.4 ± 8.1	83.5 ± 15.0
Promethazine	—	—	—	—
Group 2				
Control	23.2 ± 9.6	30.3 ± 10.9	49.4 ± 17.0	66.7 ± 10.4
Desipramine	28.1 ± 7.3	33.2 ± 6.8	29.8 ± 8.7*	37.8 ± 2.3*
Trifluoperazine	29.1 ± 7.5	37.0 ± 9.9	37.1 ± 2.33	37.1 ± 13.7*
Thiothixene	35.1 ± 13.7	39.7 ± 15.0	45.2 ± 5.1	50.9 ± 11.8
Group 3				
Control	33.4 ± 5.7	36.5 ± 9.9	58.8 ± 8.2	72.1 ± 12.2
Maprotiline	31.8 ± 12.2	33.3 ± 13.1	36.2 ± 7.4*	29.2 ± 7.5*

The BKA concentration is 10 μM, and the concentration of all of the other putative MPTP blockers is 2 μM. *, $P < 0.05$ compared with control experiment. Promethazine was toxic.

mate-induced apoptosis (Fig. 4*E*), consistent with 2-APB data (Fig. 3*D*).

Intrinsic Apoptotic Pathway, Mitochondria, and HD MSN Degeneration. Which apoptotic pathway is involved in glutamate-induced degeneration of HD MSN? Preincubation with the pan-caspase membrane-permeable inhibitor (Z-VAD-FMK), but not with the control peptide (Z-FA-FMK), reduced glutamate-induced apoptosis of YAC128 MSN to WT levels (Fig. 5*A*). Thus, apoptosis of YAC128 MSN occurs via a caspase-dependent pathway. Membrane-permeable inhibitors of caspase-3 (Z-DEVD-FMK) and caspase-9 (Z-LEHD-FMK) also protected YAC128 MSN from glutamate-induced apoptosis (Figs. 5 *B* and *C*). In contrast, a membrane-permeable inhibitor of caspase-8 (Z-IETD-FMK) was ineffective (Fig. 5*D*). These results are consistent with glutamate-induced apoptosis of YAC128 MSN occurring via the intrinsic (mitochondria and caspase-9-mediated) and not via the extrinsic (death receptor and caspase-8-mediated) pathway.

Activation of an intrinsic apoptotic pathway requires release of cytochrome *c* from the intramitochondrial space into the cytoplasm (10, 11). When WT MSN were incubated with 100 or 250 μM of glutamate for 5 h, a small elevation in cytosolic cytochrome *c* levels was observed (Fig. 5*E*). In contrast, a 5-h incubation of YAC128 MSN with 250 μM glutamate resulted in a much larger increase of cytosolic cytochrome *c* signal (Fig. 5*E*). These data are consistent with the activation of the intrinsic apoptotic pathway in YAC128 MSN but not in WT MSN, as a result of exposure to 250 μM glutamate in our experiments (Figs. 2 *A* and *B*).

Whether disturbed cytosolic Ca^{2+} signaling in YAC128 MSN (Figs. 1 *C* and *D*) is linked to the release of cytochrome *c* from the innermitochondrial space (Fig. 5*E*) is unknown. It is well established that excessive cytosolic Ca^{2+} is efficiently taken up by the mitochondria via activity of the mitochondrial Ca^{2+} uniporter/channel (MCU) located in the mitochondria inner membrane (18). Consistent with involvement of MCU in our experiments, preincubation of MSN with the membrane-permeable MCU blocker Ru360 (18, 19) reduced the glutamate-induced apoptotic cell death of YAC128 MSN to WT MSN levels (Fig. 5*F*).

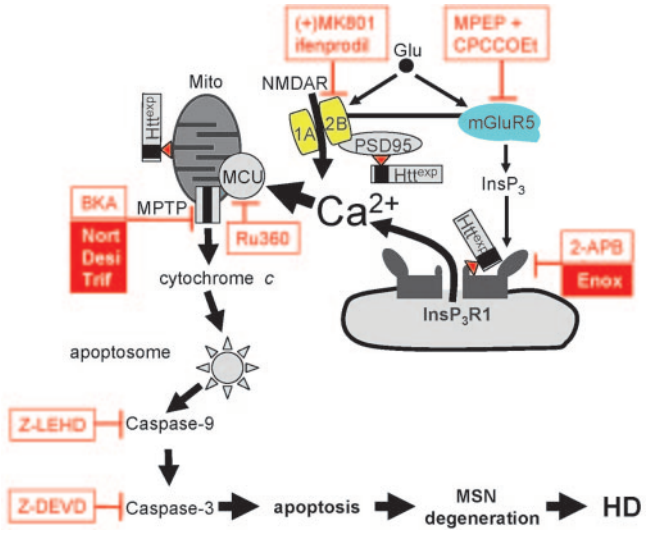

Fig. 6. Proposed mechanisms linking disturbed Ca^{2+} signaling and apoptosis of HD MSN. Glutamate released from corticostriatal projection neurons stimulates NR1A/NR2B NMDAR and mGluR5 receptors abundantly expressed in striatal MSN (22, 23). Htt^{exp} affects Ca^{2+} signaling in HD MSN by sensitizing $InsP_3R1$ to activation by $InsP_3$ (9), stimulating NR2B/NR1 NMDAR activity (6–8), and destabilizing mitochondrial Ca^{2+} handling (24, 25). As a result, stimulation of glutamate receptors leads to supranormal Ca^{2+} responses in HD MSN and mitochondrial Ca^{2+} overload. Once mitochondrial Ca^{2+} storage capacity is exceeded, the MPTP opens, leading to the release of cytochrome *c* into the cytosol and activation of caspases 9 and 3. Activation of caspase-3 leads to progression of apoptosis, MSN degeneration, and HD. The model is supported by the ability of blockers (shown in red) to reduce glutamate-induced apoptosis of YAC128 MSN to WT levels in our experiments. The blockers that were effective in our experiments are the NMDAR blocker (+)MK801 and NR2B-specific blocker ifenprodil; mGluR1/5-specific blockers MPEP and CPCCOEt; membrane-permeable $InsP_3R1$ blockers 2-APB and Enoxaparin; MCU blocker Ru360; MPTP blockers BKA, Nortriptyline, Desipramine, Trifluoperazine, and Maprotiline; membrane-permeable caspase-9 blocker Z-LEHD-FMK; and caspase-3 blocker Z-DEVD-FMK.

It has been proposed that mitochondrial Ca^{2+} overload leads to release of cytochrome *c* due to opening of the mitochondrial permeability transition pore (MPTP) (10, 11). Consistent with the role of MPTP, we demonstrated that preincubation with the 10 μM MPTP inhibitor bongkrekic acid (BKA) (20) reduced glutamate-induced apoptosis of YAC128 MSN to WT levels (Table 1). Recently, a number of biologically active Food and Drug Administration-approved heterocyclic, tricyclic, and phenothiazine-derived compounds have been identified as putative MPTP blockers (21). To determine the potential usefulness of these compounds for HD, we performed "*in vitro* HD" assay experiments with compounds from this class. We found that preincubation with 2 μM Nortriptyline, Desipramine, Trifluoperazine, or Maprotiline protected YAC128 MSN from glutamate-induced apoptosis (Table 1), consistent with their putative MPTP-blocking activity (21). As a control for specificity of observed effects, we demonstrated that Pirenzepine and Thiothixene were not protective (Table 1), despite similarity in chemical structure.

Discussion

Pathway Leading to Apoptosis of HD MSN. How polyglutamine exp in Htt^{exp} leads to neuronal death of MSN in the striatum is a central question in understanding the pathogenesis of HD (3). Our results are consistent with a model that links Htt^{exp}-induced disturbance of neuronal Ca^{2+} signaling with apoptosis of MSN

in HD (Fig. 6). Specifically, we propose that glutamate released from corticostriatal projection neurons stimulates NR1/NR2B NMDAR and mGluR5 receptors, both of which are abundantly expressed in the striatal MSN (22, 23). Activation of NR1/NR2B NMDAR leads to Ca^{2+} influx and activation of mGluR5 receptors, leading to production of $InsP_3$ and Ca^{2+} release via $InsP_3R1$ (Fig. 6). Htt^{exp} affects Ca^{2+} signaling in HD MSN by sensitizing $InsP_3R1$ to activation by $InsP_3$ (9), stimulating NR1/NR2B NMDAR activity (6–8), and directly destabilizing mitochondrial Ca^{2+} handling (24, 25). As a result, stimulation of glutamate receptors results in supranormal Ca^{2+} responses in HD MSN, leading to cytosolic Ca^{2+} overload (Fig. 6). Excessive cytosolic Ca^{2+} is taken into the mitochondria via activity of the MCU (Fig. 6). With time, mitochondrial Ca^{2+} storage capacity is exceeded, leading to an opening of MPTP, release of cytochrome *c* into the cytosol, and activation of the caspase-mediated intrinsic apoptotic program (Fig. 6). These observations suggest that delayed onset of MSN degeneration in HD is at least in part a result of significant mitochondrial Ca^{2+} storage capacity that takes a long time to exceed, as we previously speculated (12). Consistent with mitochondrial involvement is the observation of dysfunctional mitochondria in HD mouse models and in HD patients (24, 25). The abnormal cytosolic and mitochondrial Ca^{2+} levels may contribute to neurological abnormalities observed in early-grade HD patients and in HD mouse models before onset of neurodegeneration.

Potential Therapeutic Targets for Treatment of HD. The proposed model (Fig. 6) may have implications for the treatment of HD. Our results suggest that NR2B NMDAR (Fig. 3*B*) and mGluR5 (Fig. 3*A*) can be considered potential drug targets for HD treatment. We have also demonstrated that inhibition of $InsP_3R1$ by 2-APB (Fig. 3*D*), inhibition of MCU by Ru360 (Fig. 5*F*), and inhibition of MPTP by bongkrekic acid (Table 1) reduced glutamate-induced apoptosis of YAC128 MSN to WT MSN levels. Thus, $InsP_3R1$ and MPTP would appear to constitute therapeutic targets for HD. In our experiments, it was demonstrated that low-molecular-weight heparin Enoxaparin (Lovenox) exerts a neuroprotective effect on YAC128 MSN (Fig. 4*E*), apparently by directly inhibiting $InsP_3R1$ function (Figs. 4 *A–D*). Intravenous injections of Enoxaparin are neuroprotective in animal models of stroke and neurodegenerative diseases (26–28), and our results indicate that Enoxaparin may also be worthy of assessment as HD therapeutics. Recently, a number of biologically active Food and Drug Administration-approved heterocyclic, tricyclic, and phenothiazine-derived compounds have been identified as putative MPTP blockers (21). In our experiments, it is demonstrated that several members of this class of compounds (Nortriptyline, Desipramine, Trifluoperazine, and Maprotiline) protect YAC128 MSN from glutamate-induced apoptosis (Table 1). Future studies with animal models of HD or human clinical trials will be required to test the utility of putative MPTP blockers as potential therapeutics for HD. The potential side effects of these compounds, such as bleeding potential for Enoxaparin and anticholinergic actions of Nortriptyline and Desipramine, must be considered in the clinical setting.

We thank Tianhua Lei for help with maintaining the YAC mouse colony and genotyping, Linda Patterson for administrative assistance, Ethan Signer for facilitating our collaboration on MPTP blockers, and Xiaodong Wang for advice on cytochrome *c* release experiments. I.B. is supported by the Robert A. Welch Foundation, the Huntington's Disease Society of America, the Hereditary Disease Foundation, the High Q Foundation, and National Institute of Neurological Disorders and Stroke (NINDS) Grant R01 NS38082. M.R.H. is supported by the Canadian Institutes of Health Research, the Hereditary Disease Foundation, the Huntington's Disease Society of America, and the High Q Foundation, and holds a Canada Research Chair in Human Genetics. B.S.K. is supported by the Hereditary Disease Foundation and the High Q Foundation. R.L. is supported by NINDS Grant NINDS-NS13742.

1. Vonsattel, J. P. & DiFiglia, M. (1998) *J. Neuropathol. Exp. Neurol.* **57,** 369–384.
2. The Huntington's Disease Collaborative Research Group (1993) *Cell* **72,** 971–983.
3. Tobin, A. J. & Signer, E. R. (2000) *Trends Cell Biol.* **10,** 531–536.
4. Rubinsztein, D. C. (2002) *Trends Genet.* **18,** 202–209.
5. Slow, E. J., van Raamsdonk, J., Rogers, D., Coleman, S. H., Graham, R. K., Deng, Y., Oh, R., Bissada, N., Hossain, S. M., Yang, Y. Z., *et al.* (2003) *Hum. Mol. Genet.* **12,** 1555–1567.
6. Chen, N., Luo, T., Wellington, C., Metzler, M., McCutcheon, K., Hayden, M. R. & Raymond, L. A. (1999) *J. Neurochem.* **72,** 1890–1898.
7. Sun, Y., Savanenin, A., Reddy, P. H. & Liu, Y. F. (2001) *J. Biol. Chem.* **276,** 24713–24718.
8. Zeron, M. M., Hansson, O., Chen, N., Wellington, C. L., Leavitt, B. R., Brundin, P., Hayden, M. R. & Raymond, L. A. (2002) *Neuron* **33,** 849–860.
9. Tang, T.-S., Tu, H., Chan, E. Y., Maximov, A., Wang, Z., Wellington, C. L., Hayden, M. R. & Bezprozvanny, I. (2003) *Neuron* **39,** 227–239.
10. Orrenius, S., Zhivotovsky, B. & Nicotera, P. (2003) *Nat. Rev. Mol. Cell Biol.* **4,** 552–565.
11. Hajnoczky, G., Davies, E. & Madesh, M. (2003) *Biochem. Biophys. Res. Commun.* **304,** 445–454.
12. Bezprozvanny, I. & Hayden, M. R. (2004) *Biochem. Biophys. Res. Commun.* **322,** 1310–1317.
13. Hodgson, J. G., Agopyan, N., Gutekunst, C. A., Leavitt, B. R., LePiane, F., Singaraja, R., Smith, D. J., Bissada, N., McCutcheon, K., Nasir, J., *et al.* (1999) *Neuron* **23,** 181–192.
14. Lupu, V. D., Kaznacheyeva, E., Krishna, U. M., Falck, J. R. & Bezprozvanny, I. (1998) *J. Biol. Chem.* **273,** 14067–14070.
15. Tang, T. S., Tu, H., Orban, P. C., Chan, E. Y., Hayden, M. R. & Bezprozvanny, I. (2004) *Eur. J. Neurosci.* **20,** 1779–1787.
16. Maruyama, T., Kanaji, T., Nakade, S., Kanno, T. & Mikoshiba, K. (1997) *J. Biochem. (Tokyo)* **122,** 498–505.
17. Jonas, S., Sugimori, M. & Llinás, R. (1997) *Ann. N.Y. Acad. Sci.* **825,** 389–393.
18. Kirichok, Y., Krapivinsky, G. & Clapham, D. E. (2004) *Nature* **427,** 360–364.
19. Ying, W. L., Emerson, J., Clarke, M. J. & Sanadi, D. R. (1991) *Biochemistry* **30,** 4949–4952.
20. Halestrap, A. P., McStay, G. P. & Clarke, S. J. (2002) *Biochimie* **84,** 153–166.
21. Stavrovskaya, I. G., Narayanan, M. V., Zhang, W., Krasnikov, B. F., Heemskerk, J., Young, S. S., Blass, J. P., Brown, A. M., Beal, M. F., Friedlander, R. M. & Kristal, B. S. (2004) *J. Exp. Med.* **200,** 211–222.
22. Landwehrmeyer, G. B., Standaert, D. G., Testa, C. M., Penney, J. B., Jr., & Young, A. B. (1995) *J. Neurosci.* **15,** 5297–5307.
23. Testa, C. M., Standaert, D. G., Landwehrmeyer, G. B., Penney, J. B., Jr., & Young, A. B. (1995) *J. Comp. Neurol.* **354,** 241–252.
24. Panov, A. V., Gutekunst, C. A., Leavitt, B. R., Hayden, M. R., Burke, J. R., Strittmatter, W. J. & Greenamyre, J. T. (2002) *Nat. Neurosci.* **5,** 731–736.
25. Choo, Y. S., Johnson, G. V., MacDonald, M., Detloff, P. J. & Lesort, M. (2004) *Hum. Mol. Genet.* **13,** 1407–1420.
26. Stutzmann, J. M., Mary, V., Wahl, F., Grosjean-Piot, O., Uzan, A. & Pratt, J. (2002) *CNS Drug Rev.* **8,** 1–30.
27. Mary, V., Wahl, F., Uzan, A. & Stutzmann, J. M. (2001) *Stroke* **32,** 993–999.
28. Bergamaschini, L., Rossi, E., Storini, C., Pizzimenti, S., Distaso, M., Perego, C., De Luigi, A., Vergani, C. & De Simoni, M. G. (2004) *J. Neurosci.* **24,** 4181–4186.